Computation of Switch Time Distributions in Stochastic Gene Regulatory Networks

Brian Munsky and Mustafa Khammash
Center for Control, Dynamical Systems and Computation
University of California
Santa Barbara, CA 93106-5070

***Abstract*— Many gene regulatory networks are modeled at the mesoscopic scale, where chemical populations are assumed to change according a discrete state (jump) Markov process. The chemical master equation (CME) for such a process is typically infinite dimensional and is unlikely to be computationally tractable without further reduction. The recently proposed Finite State Projection (FSP) technique allows for a bulk reduction of the CME while explicitly keeping track of its own approximation error. In previous work, this error has been reduced in order to obtain more accurate CME solutions for many biological examples. In this paper, we show that this "error" has far more significance than simply the distance between the approximate and exact solutions of the CME. In particular, we show that apart from its use as a measure for the quality of approximation, this error term serves as an exact measure of the rate of first transition from one system region to another. We demonstrate how this term may be used to directly determine the statistical distributions for stochastic switch rates, escape times, trajectory periods, and trajectory bifurcations. We illustrate the benefits of this approach to analyze the switching behavior of a stochastic model of Gardner's genetic toggle switch.**

I. Introduction

The majority of modeling and analysis of biological systems is done using ordinary differential equations (ODEs). In biochemical systems these equations depend upon assumptions that (1) the system contains so many molecules that each chemical can be described with a continuous valued concentration, and (2) that the system behaves at thermal equilibrium. Under these assumptions of mass action kinetics, the resulting ODE models can be analyzed using efficient and accurate numerical integration software. However, for many gene regulatory networks, some chemical species are so rare that they must be quantified by discrete integer amounts. These rare chemical species may include crucial cellular components such as genes, RNA molecules, and proteins, which can in turn affect a vast array of biological functions. As a result, a slightly noisy environment will introduce significant randomness and result in phenomena such as stochastic switching [1], stochastic focussing [2], stochastic resonance, and other effects. These effects cannot be captured with deterministic models, and require a separate set of analytical tools.

Gillespie showed in [3] that if a chemical system is well mixed and kept at constant temperature and volume, then that system behaves as a discrete state Markov process. Each state of this process corresponds to a specific population vector, and each jump is a reaction that takes the system from one population vector to another. The probability distribution of such a chemical process evolves according to a set of linear ODEs known as the chemical master equation (CME). Although the CME is relatively easy to define (see below), it can be very difficult or impossible to solve exactly. For this reason, most research on the CME has concentrated on simulating trajectories of the CME using methods such as the Stochastic Simulation Algorithm (SSA) [4] or one of its various approximations (see for example: [5], [6]). While these methods reliably provide samples of the process defined by the CME, they require a huge collection of simulations to obtain an accurate statistical solution. This becomes particularly troublesome, when one wishes to compute the transition probabilities of very rare events or to compare distributions arising from slightly different parameter sets.

Recently, we developed a new approach to obtain an approximate solution to the CME: the Finite State Projection (FSP) algorithm [7]–[10]. This approach systematically collapses the infinite state Markov process into a combination of a truncated finite state process and a single absorbing "error sink". The resulting system is finite dimensional and solvable. The probabilities of the truncated process give a lower bound approximation to the true CME solution. The probability measure of the error sink gives an exact computation of the error in this approximation. This error can then be decreased to reach any non-zero error tolerance through a systematic expansion of projections known as the FSP algorithm [7]. However, as we will illustrate in this paper, the "error" guarantee of the FSP provides more than a simple distance between the FSP solution and the true solution to the CME. Instead, this important term in the projection provides a wealth of additional information about the Markov process. From it one can determine the statistical distributions of switch rates and escape probabilities and also analyze stochastic pathway bifurcation decisions.

The focus of this paper is to explore this added information contained in the FSP "error" term and to present some of the types of analyses for which this information provides. The next section will provide a precise summary of the original FSP results from [7] but with an emphasis on the understanding of the underlying intuition of the error sink. In Section III, we show how this sink can be used to determine some statistical quantities for stochastic switches, such as switch waiting and return times. Section IV will then show

how multiple absorbing sinks can be used to effectively analyze pathway bifurcation decisions in stochastic systems. In Section V we will illustrate how these new approaches can be applied to a stochastic model of the genetic toggle switch [11]. Finally, in Section VI we will finish with some concluding remarks.

II. Background on the Finite State Projection approach

For many biochemical systems, it is convenient to assume that all of the microscopic dynamics–intermolecular forces and collisions, changing molecular geometries, thermal fluctuations, and so forth–all average out to yield a far simpler jump Markov process. Indeed such assumptions are well supported in the case of a fixed volume, fixed temperature, well-mixed, reaction of ideal gasses as shown by Gillespie in [3]. This scale is commonly referred to as the *mesoscopic* scale of chemical kinetics.

In the mesoscopic description of chemical kinetics the state of an N reactant process is defined by the integer population vector $\mathbf{x} \in \mathbb{Z}^N$. Reactions are transitions from one state to another $\mathbf{x} \to \mathbf{x} + \nu_\mu$, where ν_μ is known as the stoichiometry (or direction of transition) of the μ^{th} reaction. For any $\mathbf{x}_i$ there are at most M reactions that will take the system from $\mathbf{x}_i$ to some other state $\mathbf{x}_j \neq \mathbf{x}_i$ and at most M reactions that will bring the system from $\mathbf{x}_k \neq \mathbf{x}_i$ to $\mathbf{x}_i$. Each reaction has an infinitesimal probability of occurring in the next infinitesimal time step of length dt; this quantity is known as the propensity function: $w_\mu(\mathbf{x})dt$.

If $P_i(t)$ and $P_i^\mu(t)$ are used to denote the probabilities that the system will be in $\mathbf{x}_i$ and $\mathbf{x}_i^\mu = \mathbf{x}_i - \nu_\mu$, respectively, at time t, then:

$$\frac{P_i(t+dt) - P_i(t)}{dt} = -\sum_{\mu=1}^{M} w_\mu(\mathbf{x}_i)P_i(t) - w_\mu(\mathbf{x}_i^\mu)P_i^\mu(t).$$

Taking the limit $dt \to 0$ easily yields the chemical master equation, which can be written in vector form as: $\dot{\mathbf{P}}(t) = \mathbf{A}\mathbf{P}(t)$. The ordering of the infinitesimal generator, $\mathbf{A}$, is determined by the enumeration of the configuration set $\mathbf{X} = \{\mathbf{x}_1, \mathbf{x}_2, \mathbf{x}_3, \ldots\}$. Each i^{th} diagonal element of $\mathbf{A}$ is negative with a magnitude equal to the sum of the propensity functions of reactions that *leave* the i^{th} configuration. Each off-diagonal element, A_{ij}, is positive with magnitude $w_\mu(\mathbf{x}_j)$ if there is a reaction $\mu \in \{1, \ldots, M\}$ such that $\mathbf{x}_i = \mathbf{x}_j + \nu_\mu$ and zero otherwise. In other words:

$$\mathbf{A}_{ij} = \left\{ \begin{array}{ll} -\sum_{\mu=1}^{M}(w_\mu(\mathbf{x}_i)) & \text{for } (i=j) \\ w_\mu(\mathbf{x}_j) & \text{for all } j \text{ such that } (\mathbf{x}_i = \mathbf{x}_j + \nu_\mu) \\ 0 & \text{Otherwise} \end{array} \right\}. \tag{1}$$

When the cardinality of the set $\mathbf{X}$ is infinite or extremely large, the solution to the CME is unclear or vastly difficult to compute, but one can get a good approximation of that solution using Finite State Projection (FSP) techniques [7]–[10]. To review the FSP, we will first introduce some convenient notation. Let $J = \{j_1, j_2, j_3, \ldots\}$ denote an index set, and let J' denote the complement of the set J. If $\mathbf{X}$ is an enumerated set $\{\mathbf{x}_1, \mathbf{x}_2, \mathbf{x}_3, \ldots\}$, then $\mathbf{X}_J$ denotes the subset $\{\mathbf{x}_{j_1}, \mathbf{x}_{j_2}, \mathbf{x}_{j_3}, \ldots\}$. Furthermore, let $\mathbf{v}_J$ denote the subvector of $\mathbf{v}$ whose elements are chosen according to J, and let $\mathbf{A}_{IJ}$ denote the submatrix of $\mathbf{A}$ such that the rows have been chosen according to I and the columns have been chosen according to J. For example, if I and J are defined as $\{3,1,2\}$ and $\{1,3\}$, respectively, then:

$$\begin{bmatrix} a & b & c \\ d & e & f \\ g & h & k \end{bmatrix}_{IJ} = \begin{bmatrix} g & k \\ a & c \\ d & f \end{bmatrix}.$$

For convenience, let $\mathbf{A}_J := \mathbf{A}_{JJ}$.

Let $\mathcal{M}$ denote a Markov chain on the configuration set $\mathbf{X}$, such as that shown in Fig. 1(a), whose master equation is $\dot{\mathbf{P}}(t) = \mathbf{A}\mathbf{P}(t)$, with initial distribution $\mathbf{P}(0)$. Let $\mathcal{M}_J$ denote a reduced Markov chain, such as that in Fig. 1(b), comprised of the configurations indexed by J plus a single absorbing state. The master equation of $\mathcal{M}_J$ is given by

$$\begin{bmatrix} \dot{\mathbf{P}}_J^{FSP}(t) \\ \dot{G}(t) \end{bmatrix} = \begin{bmatrix} \mathbf{A}_J & \mathbf{0} \\ -\mathbf{1}^T\mathbf{A}_J & 0 \end{bmatrix} \begin{bmatrix} \mathbf{P}_J^{FSP}(t) \\ G(t) \end{bmatrix}, \tag{2}$$

with initial distribution,

$$\begin{bmatrix} \mathbf{P}_J^{FSP}(0) \\ G(0) \end{bmatrix} = \begin{bmatrix} \mathbf{P}_J(0) \\ 1 - \sum \mathbf{P}_J(0) \end{bmatrix}.$$

At this point it is crucial to have a very clear understanding of how the process $\mathcal{M}_J$ relates to $\mathcal{M}$ and in particular the definitions of the terms $\mathbf{P}_J^{FSP}(t)$ and $G(t)$. First, the scalar $G(0)$ is the exact probability that the system begins in the set $\mathbf{X}_{J'}$ at time $t = 0$, and $G(t)$ is the exact probability that the system has been in the set $\mathbf{X}_{J'}$ at *any* time $\tau \in [0, t]$. Second, the vector $\mathbf{P}_J^{FSP}(0)$ contains the exact probabilities that the system begins in the set $\mathbf{X}_J$ at time $t = 0$, and $\mathbf{P}_J^{FSP}(t)$ are the exact *joint* probabilities that the system (*i*) is in the corresponding states $\mathbf{X}_J$ at time t, and (*ii*) the system has remained in the set $\mathbf{X}_J$ *for all* $\tau \in [0, t]$.

With this understanding, the relevant portions of the original FSP theorems [7] are trivial to state and to prove as follows:

Theorem 1. For any index set J and any initial distribution $\mathbf{P}(0)$, it is guaranteed that

$$\mathbf{P}_J(t) \geq \mathbf{P}_J^{FSP}(t) \geq \mathbf{0}.$$

Proof. $\mathbf{P}_J^{FSP}(t)$ is a more restrictive joint distribution than $\mathbf{P}_J(t)$.

Theorem 2. Consider any Markov chain $\mathcal{M}$ and its reduced Markov chain $\mathcal{M}_J$. If $G(t_f) = \varepsilon$, then

$$\left\| \begin{bmatrix} \mathbf{P}_J(t_f) \\ \mathbf{P}_{J'}(t_f) \end{bmatrix} - \begin{bmatrix} \mathbf{P}_J^{FSP}(t_f) \\ \mathbf{0} \end{bmatrix} \right\|_1 = \varepsilon. \tag{3}$$

Proof. The left side of (3) can be expanded to:

$$LHS = \left\|\mathbf{P}_J(t_f) - \mathbf{P}_J^{FSP}(t_f)\right\|_1 + \left\|\mathbf{P}_{J'}(t_f)\right\|_1.$$

Applying the Theorem 1 yields

$$LHS = \left\|\mathbf{P}_J(t_f)\right\|_1 - \left\|\mathbf{P}_J^{FSP}(t_f)\right\|_1 + \left\|\mathbf{P}_{J'}(t_f)\right\|_1.$$

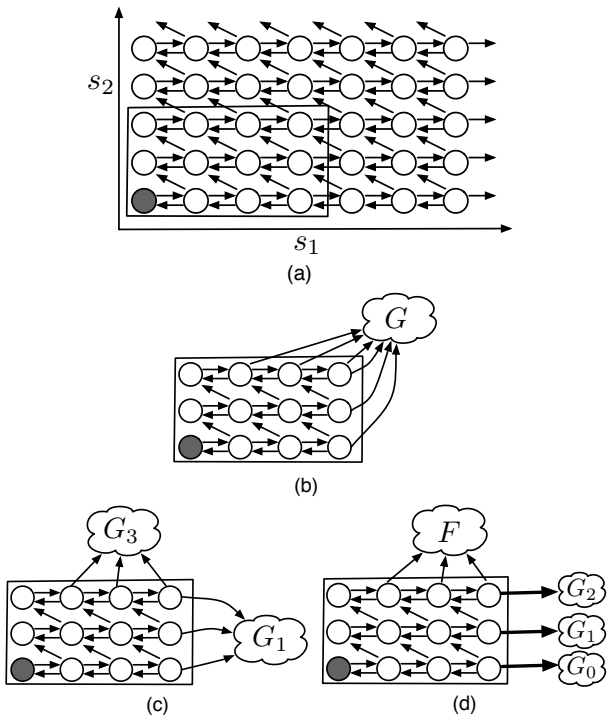

Fig. 1. (a): A Markov chain for a two species chemically reacting system, $\mathcal{M}$. The process begins in the configuration shaded in grey and undergoes three reactions: The first reaction $\emptyset \rightarrow s_1$ results in a net gain of one s_1 molecule and is represented by right arrows. The second reaction $s_1 \rightarrow \emptyset$ results in a net loss of one s_1 molecule and is represented by a left arrow. The third reaction $s_1 \rightarrow s_2$ results in a loss of one s_1 molecule and a gain of one s_2 molecule. The dimension of the Master equation is equal to the total number of configurations in $\mathcal{M}$, and is too large to solve exactly. (b) In the FSP algorithm a configuration subset, $\mathbf{X}_J$ is chosen and all remaining configurations are projected to a single absorbing point, G. This results in a small dimensional Markov process, $\mathcal{M}_J$. (c,d) Instead of considering only a single absorbing point, transitions out of the finite projection can be sorted as to how they leave the projection space. (c) G_1 and G_3 absorb the probability that has leaked out through reactions 1 or 3, respectively. This information can then be used to analyze the probabilities of certain decisions or to expand the configuration set in later iterations of the FSP algorithm. (d) Each G_i absorbs the probability that s_1 first exceeds a certain threshold, s_1^{max} when $s_2 = i$.

Since $\mathbf{P}(t_f)$ is a probability distribution $|\mathbf{P}_J(t_f)|_1 + |\mathbf{P}_{J'}(t_f)|_1 = |\mathbf{P}(t_f)|_1 = 1$ and the LHS can be rewritten:

$$LHS = 1 - \left|\mathbf{P}_J^{FSP}(t_f)\right|_1.$$

Because the pair $\{G(t_f), \mathbf{P}_J^{FSP}(t_f)\}$ are a probability distribution for $\mathcal{M}_J$, one can see that the right hand side is precisely equal to $|G(t_f)|_1$ and the proof is complete.

Theorem 1 guarantees that as we add points to the subset $\mathbf{X}_J$, then the $\mathbf{P}_J^{FSP}(t_f)$, monotonically increases, and Theorem 2 provides a certificate of how close the approximation is to the true solution.

In previous work, the probability lost to the absorbing state, $G(t)$, has been used only as in Theorem 2 as a means to evaluate the FSP projection in terms of its accuracy compared to the true CME solution. As a probability of first transition, however, this term has an importance of its own, as we will see in the remainder of this paper.

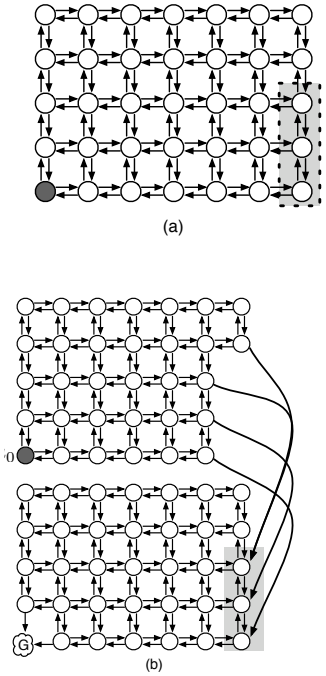

Fig. 2. Schematic representation for the computation of round trip times for discrete state Markov processes. (a) A Markov chain, $\mathcal{M}$ where the system begins in the shaded circle, and we wish to find the distribution for the time at which the system first enters then shaded region and then returns to the initial state. (b) A corresponding Markov process where the top points correspond to states on the journey from the dark circle to the shaded box, and the bottom circles correspond to states along the return trip. In this description, the absorbing point $G(t)$ corresponds to the probability that the system has gone from the initial condition to the grey box and then back again.

III. Analyzing switch statistics with the FSP

As discussed above, the term $G(t)$ for the process $\mathcal{M}_J$ is simply the probability that the system has escaped from $\mathbf{X}_J$ at least once in the time interval $[0, t]$. With such an expression, it is almost trivial to find quantities such as median or p^{th} percentile escape times from the set $\mathbf{X}_J$. We need only find the time t such that $G(t)$ in (2) is equal to $p\%$. In other words, we find t such that

$$G(t) = 1 - |\exp(\mathbf{A}_J t)\mathbf{P}_J(0)|_1 = 0.01p. \tag{4}$$

This can be solved with a relatively simple line search as we will do in the example of Section V. Using a multiple time interval FSP approach such as those explored in [9] or [10] could significantly speed up such a search, but this has not been utilized in this study.

Alternatively, one may wish to ask not only for escape times, but for the periods required to complete more complicated trajectories. For example, suppose the we have a Markov chain such as that in Fig. 2(a). The system begins in the state represented by the shaded circle, and we wish to know the distribution for the time until the system will first visit the region in the grey box and then return to the original state. Biologically this may correspond to the probability that a system will switch from one phenotypical expression to another and then back again. To solve this problem, we can duplicate the lattice as shown in Fig. 2(b).

In this description, the top lattice corresponds to states where the system has never reached the grey box, and the bottom lattice corresponds to states where the system has first passed through that box. The master equation for this system is given by:

$$\begin{bmatrix} \dot{\mathbf{P}}^1_{J_1}(t) \\ \dot{\mathbf{P}}^2_{J_2}(t) \\ \dot{G}(t) \end{bmatrix} = \begin{bmatrix} \mathbf{A}_{J_1} & \mathbf{0} & \mathbf{0} \\ \mathbf{C} & \mathbf{A}_{J_2} & \mathbf{0} \\ \mathbf{0} & -\mathbf{1}^T\mathbf{A}_{J_2} & \mathbf{0} \end{bmatrix} \begin{bmatrix} \mathbf{P}^1_{J_1}(t) \\ \mathbf{P}^2_{J_2}(t) \\ G(t) \end{bmatrix}, \quad (5)$$

where $\mathbf{X}_{J_1}$ includes every state except those in the grey box, and $\mathbf{X}_{J_2}$ includes every state except the final destination. The matrix $\mathbf{C}$ accounts for transitions that begin in $\mathbf{X}_{J_1}$ and end in $\mathbf{X}_{J_2}$ (via a transition into the grey box) and can be expressed:

$$\mathbf{C}_{ik} = \left\{ \begin{array}{ll} w_\mu(\mathbf{x}_k) & \text{for } \mathbf{x}_k \in \mathbf{X}_{J_1} \text{ and} \\ & \mathbf{x}_k + \nu_\mu = \mathbf{x}_i \in \mathbf{X}_{J_2} \\ 0 & \text{Otherwise} \end{array} \right\}. \quad (6)$$

The initial distribution is simply $[1, 0, \ldots, 0]^T$. The probability of the absorbing point, $G(t)$, in this description is now exactly the probability that the system has completed the return trip in the time interval $[0, t]$. This solution scheme requires a higher dimensional problem than the original problem. However, with the FSP approach from [7], this dimension could be reduced while maintaining a measure of the method's accuracy. As an approximate alternative to duplicating the system and solving such a high dimensional problem, one can utilize the linearity of the system to solve the problem with a numerical convolution approach, as is shown in an extended version of this article [12].

IV. Pathway Bifurcation analysis with the FSP

There are numerous examples in which biological systems decide between expressing two or more vastly different responses. These decisions occur in developmental pathways in multicellular organisms as heterogeneous cells divide and differentiate, in single cell organisms that radically adapt to survive or compete in changing environments, and even in viruses that must decide to lay dormant or make copies of themselves and ultimately destroy their host [1]. Many of these decisions are stochastic in nature, and models and methods are needed to determine the nature and probability of these decisions. Next, we show how the FSP approach can be adapted to answer some of these questions.

In the original FSP approach, a single absorbing state has been used, whose probability coincides with the probability that the system has exited the region $\mathbf{X}_J$. Suppose one wishes to know a little more about *how* the system has exited this region. For example in the process in Fig. 1(a), one may ask:

Problem 1: What is the probability that the system leaves $\mathbf{X}_J$ via reaction 1 (rightward horizontal arrow) or via reaction 3 (leftward diagonal arrow)?

Problem 2: What is the probability distribution for the population of species s_2 when the population of s_1 first exceeds a specific threshold, s_1^{max}?

These questions can be answered by creating a new Markov process with multiple absorbing states as shown in Fig. 1(c,d). Let $\mathcal{M}^*_J$ refer to such a chain where we have included K different absorbing states. The CME for the two problems above can be written as:

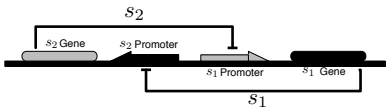

Fig. 3. Schematic of the toggle model comprised of two inhibitors: s_1 inhibits the production of s_2 and vice-versa.

$$\begin{bmatrix} \dot{\mathbf{P}}^{FSP}_J(t) \\ \dot{\mathbf{G}}(t) \end{bmatrix} = \begin{bmatrix} \mathbf{A}_J & \mathbf{0} \\ \mathbf{Q} & \mathbf{0} \end{bmatrix} \begin{bmatrix} \mathbf{P}^{FSP}_J(t) \\ \mathbf{G}(t) \end{bmatrix}, \quad (7)$$

where $\mathbf{G} = [G_0, \ldots, G_K]^T$ and the matrix $\mathbf{Q}$ is given in Problem 1 by:

$$\mathbf{Q}_{\mu i} = \left\{ \begin{array}{cc} a_\mu(\mathbf{x}_{j_i}) & \text{if } (\mathbf{x}_{j_i} + \nu_\mu) \notin \mathbf{X}_J \\ 0 & \text{Otherwise} \end{array} \right\},$$

and in Problem 2 by:

$$\mathbf{Q}_{ki} = \left\{ \begin{array}{cc} \sum a_\mu(\mathbf{x}_{j_i}) & \text{For all } j_i \text{ s.t. } (\mathbf{x}_{j_i})_2 = k \\ & \text{and } \mu \text{ s.t. } (\mathbf{x}_{j_i} + \nu_\mu)_1 > s_1^{max} \\ 0 & \text{Otherwise} \end{array} \right\}.$$

Note the underlying requirement that each j_i is an element of the index set J. Also recall that $\mathbf{x}_j$ is a population vector–the integer $(\mathbf{x}_j)_n$ is the n^{th} element of that population vector.

For either problem, the solution of (7) at a time t_f is found by taking the exponential of the matrix in (7) and has the form

$$\begin{bmatrix} \mathbf{P}^{FSP}_J(t) \\ \mathbf{G}(t) \end{bmatrix} = \begin{bmatrix} \exp(\mathbf{A}_J t_f) & \mathbf{0} \\ \int_0^{t_f} \mathbf{Q}\exp(\mathbf{A}_J\tau)d\tau & \mathbf{I} \end{bmatrix} \begin{bmatrix} \mathbf{P}^{FSP}_J(0) \\ \mathbf{G}(0) \end{bmatrix}. \quad (8)$$

This solution yields all of the same information as previous projections with regards to the accuracy of $\mathbf{P}^{FSP}_J(t)$, but it now provides additional useful knowledge. Specifically, each $G_k(t)$ gives the cumulative probability distribution at time t that the system will have exited from $\mathbf{X}_J$ at least once and that that exit transition will have occurred in the specific manner that was used to define the k^{th} absorbing state.

In [7] we showed a FSP algorithm that relied on increasing the set $\mathbf{X}_J$ until the solution reaches a certain pre-specified accuracy. The additional knowledge gained from solving Problems 1 or 2 above is easily incorporated into this algorithm. If most of the probability measure left via one particular reaction or from one particular region of $\mathbf{X}_J$, it is reasonable to expand $\mathbf{X}_J$ accordingly. Such an approach is far more efficient that the original FSP algorithm and has been considered in [9].

V. Analyzing the genetic toggle switch

To illustrate the usefulness of the absorbing sink of the FSP in the analysis of stochastic gene regulatory networks, we consider a stochastic model of the Gardner's gene toggle model [11]. This system, shown in Fig. 3 is comprised of two mutually inhibiting proteins, s_1 and s_2. The four reactions, R_μ, and corresponding propensity functions, w_μ, are given as:

R_1	;	R_2	;	R_3	;	R_4
$\emptyset \rightarrow s_1$	;	$s_1 \rightarrow \emptyset$	;	$\emptyset \rightarrow s_2$	;	$s_2 \rightarrow \emptyset$
$w_1 = \frac{16}{1+s_2}$	;	$w_2 = s_1$	;	$w_3 = \frac{50}{1+s_1^{2.5}}$	;	$w_4 = s_2$

For these parameters, the system exhibits two distinct phenotypes, which for convenience we will label OFF and ON. By definition, we will call the cell OFF when the population of s_1 exceeds 5 molecules, and we will label the system as being ON when the population of s_2 exceeds 15 molecules. Each of these phenotypes is relatively stable–once the system reaches the ON or OFF state, it tends to stay there for some time. For this study, we assume that the system begins with a population $s_1 = s_2 = 0$, and we wish to analyze the subsequent switching behavior.

Q1. *After the process starts, the system will move within its configuration space until eventually s_1 exceeds 5 molecules (the cell turns OFF) or s_2 exceeds 15 molecules (the cell turns ON). What percentage will choose to turn ON first (s_2 exceeds 15* before *s_1 exceeds 5)?*

To analyze this initial switch decision, we use the methodology outlined in Section IV. We choose $\mathbf{X}_J$ to include all states such that $s_1 \leq 5$ and $s_2 \leq 15$. There are only two means through which the system may exit this region: If $s_1 = 5$ and R_1 occurs (making $s_1 = 6$), then the system is absorbed into a sink state G_{OFF}. If $s_2 = 15$ and R_3 occurs, then the system is absorbed into a sink state G_{ON}. The master equation for this Markov chain has the form of that in (7) and contains 98 states including the two absorbing sinks. By solving this equation for the given initial condition, one can show that the probability of turning ON first is 78.1978%. Thus, nearly four-fifths of the cells will turn ON before they turn OFF. The asymptotes of the blue and red dashed lines in Fig. 4(bottom) correspond to the probabilities of that the system will first turn ON and OFF, respectively.

Q2. *Find the times t_{50} and t_{99} at which 50% and 99% of all cells will have made their initial decision to turn ON or OFF?*

To solve this question we can use the same Markov chain as in Q1, and search for the times, t_{50} and t_{99}, at which $G_{OFF}(t_{50}) + G_{ON}(t_{50}) = 0.5$ and $G_{OFF}(t_{99}) + G_{ON}(t_{99}) = 0.99$, respectively. This has been done using a simple line search, in which we found that $t_{50} = 0.5305s$ and $t_{99} = 5.0595s$. In Fig 4(bottom) these times would correspond to the point in time where the black dashed line cross 0.5 and 0.99, respectively.

Q3. *What is the time at which 99% of all cells will have turned ON at least once?*

Because we must include the possibility that the cell will first turn OFF and then turn ON, this solution for this question requires a different projection. We have chosen to use a projection, $\mathbf{X}_{J_1}$, that includes all states such that $s_1 \leq 45$ and $s_2 \leq 15$. There are only two means through which the system may exit this region: G_{ON} is basically the same as above. However, the system can still exit $\mathbf{X}_{J_1}$ if $s_1 = 45$ and R_1 occurs; in this case the probability is absorbed into a sink state G_{err}, which will result in a loss of precision in our results. This error comes into play as follows: If t_1 is defined as the time at which $G_{ON}(t_1) + G_{err}(t_1) = 0.99$, and t_2 is defined as the time at which $G_{ON}(t_2) = 0.99$, then the time, t_{99}, at which 99% turn ON is bounded by $t_1 \leq t_{99} \leq t_2$. For the chosen projection, this bound is very tight yielding a guarantee that $t_{99} \in [1733.1, 1733.2]s$. Similarly, one can use a projection, $\mathbf{X}_{J_2}$ where $s_1 \leq 5$ and $s_2 \leq 100$ to find that it will take between 798.468 and 798.472 seconds until 99% of cells will turn OFF.

Note that the times for Q3 are very large in comparison to those in Q2; this results from the fact that the ON and OFF regions are relatively stable. This trait is evident in Fig. 4. In the figure, the blue dashed line corresponds to the time of the first ON decision *provided that the system has not previously turned OFF*. Since only about 78% percent decide to turn ON before they turn OFF, this curve asymptotes at about 0.78 (see Q1 and Q2). On the other hand, the solid blue line corresponds to the times for the first ON decision *whether or not the system has previously turned OFF*. The red curves represent the same information for the OFF decisions. The kinks in these distributions, where the solid and dashed curves separate, result from the stability of the OFF region. In particular, the curve for the first switch to the ON state exhibits a more severe kink due to the fact that the OFF region is more stable than the ON region (compare solid red line to solid blue line).

Q4. *What is the distribution for the round trip time until a cell will first turn ON and then turn OFF?*

In order to answer this question we use the round-trip methodology from the latter half of Section III. Intuitively, this approach is very similar to that depicted in Fig. 2(bottom), except that now the top and bottom portions of the Markov chain are not identical and the final destination is a region of the chain as opposed to a single point. Also, since the Markov process under examination is infinite dimensional, we will apply a finite state projection to reduce this system to a finite set. For the system's outbound journey into the ON region, we use the projection $\mathbf{X}_{J_1}$ from Q3 where $s_1 \leq 45$ and $s_2 \leq 15$. After the system turns ON, it begins the second leg of its trip to the OFF region through a different projection $\mathbf{X}_{J_2}$ where $s_1 \leq 5$ and $s_2 \leq 100$. When the system reaches the OFF region on the second leg, it is absorbed into a sink $G(t)$. The transition from the set $\mathbf{X}_{J_1}$ to $\mathbf{X}_{J_2}$ occurs only when the system is in one of the states $[s_1, s_2] \in \{[0, 15], [1, 15], \ldots, [5, 15]\}$. The full master equation for this process can be written as:

$$\begin{bmatrix} \dot{\mathbf{P}}^1_{J_1}(t) \\ \dot{\mathbf{P}}^2_{J_2}(t) \\ \dot{G}(t) \\ \dot{\varepsilon}(t) \end{bmatrix} = \begin{bmatrix} \mathbf{A}_{J_1} & \mathbf{0} & \mathbf{0} & \mathbf{0} \\ \mathbf{C}_{21} & \mathbf{A}_{J_2} & \mathbf{0} & \mathbf{0} \\ \mathbf{0} & \mathbf{c}_{32} & 0 & 0 \\ \mathbf{c}_{\varepsilon 1} & \mathbf{c}_{\varepsilon 2} & 0 & 0 \end{bmatrix} \begin{bmatrix} \mathbf{P}^1_{J_1}(t) \\ \mathbf{P}^2_{J_2}(t) \\ G(t) \\ \varepsilon(t) \end{bmatrix}, \quad (9)$$

where $\mathbf{A}_{J_1}$ and $\mathbf{A}_{J_2}$ are defined as in (1). The matrix $\mathbf{C}_{21}$ is defined as in (6) and accounts for the transitions from the states $[s_1, s_2] = \{[0, 15], [1, 15], \ldots, [5, 15]\} \in \mathbf{X}_{J_1}$ to the corresponding states $[s_1, s_2] = \{[0, 16], [1, 16], \ldots, [5, 16]\} \in \mathbf{X}_{J_2}$. The vector $\mathbf{c}_{32}$ corresponds to the transitions that exit $\mathbf{X}_{J_2}$ and

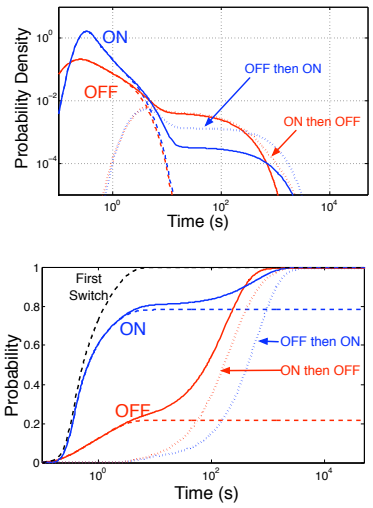

Fig. 4. Probability densities (top) and cumulative distributions (bottom) of the times of switch decisions for a stochastic model of Gardner's gene toggle switch [11]. The blue and red dashed lines correspond to the probabilities that the first switch decision will be to enter the ON or OFF region, respectively. Note that the system will turn ON first for about 78% of trajectories (Q1); the rest will turn OFF first (see asymptotes of dashed lines in bottom plot). The black dashed line in the bottom plot is equal to the sum of the red and blue dashed lines; this corresponds to the cumulative distribution until the time of the first switch decision (Q2). The solid lines correspond to the probabilities for the first time the system will reach the ON (or OFF) region (Q3). The dotted lines correspond to the times until the system completes a trajectory in which it begins at $s_1 = s_2 = 0$, it turns ON (or OFF), and finally turns OFF (or ON) (Q4).

turn OFF (completing the full trip). The last two vectors $\mathbf{c}_{\varepsilon 1}$ and $\mathbf{c}_{\varepsilon 2}$ correspond to the rare transitions that leave the projected space and therefore contribute to a computable error, $\varepsilon(t)$ in our analysis.

The solution of this system for the scalar $G(t)$ then gives us the joint probability that (*i*) the system remains in the set $\mathbf{X}_{J_1}$ until it enters the ON region at some time $\tau_1 \in [0, t)$, and (*ii*) it then remains in the set $\mathbf{X}_{J_2}$ until it enters the OFF region at some time $\tau_2 \in (\tau_1, t]$. This distribution is plotted with the dotted lines in Fig. 4. Once again we can see the effect that the asymmetry of the switch plays on the times of these trajectories; the ON region is reached first more often and the ON region is less stable, thus the ON then OFF trajectory will occur significantly faster than the OFF then ON trajectory (compare red and blue dotted lines in Fig. 4).

VI. Conclusion

In order to account for the importance of intrinsic noise, researchers model many gene regulatory networks as being jump Markov processes. In this description, each state corresponds to a specific integer population vector and transitions correspond to individual reactive events. These processes have probability distributions that evolve according to a possibly infinite dimensional chemical master equation (CME) [3]. In previous work, we showed that the Finite State Projection (FSP) method [7] can provide a very accurate solution to the CME for some stochastic gene regulatory networks. The FSP method works by choosing a small finite set of possible states and then keeping track of how much of the probability measure exits that set as time passes. In the original FSP, the amount of the probability measure that exits the chosen region yields bounds on the FSP approximation error. In this paper we have shown that this exit probability has intrinsic value and can allow for the precise computation of the statistics of switching times, escape times and completion times for certain more involved trajectories. We have illustrated these techniques on a stochastic model of Gardner's genetic toggle switch [11]. We have used the FSP to find the distribution for the times at which the system first turns ON or OFF as well as the time until the system will complete a trajectory in which it first switches one way and then the other. In each of these computations, the FSP results come with extremely precise guarantees as to their own accuracy.

Acknowledgment

The authors would like to acknowledge Eric Klavins, with whom we have many interesting discussions on related topics. This material is based upon work supported by the National Science Foundation under Grant NSF-ITR CCF-0326576 and the Institute for Collaborative Biotechnologies through Grant DAAD19-03-D-0004 from the U.S. Army Research Office.

References

[1] A. Arkin, J. Ross, and M. H., "Stochastic kinetic analysis of developmental pathway bifurcation in phage λ-infected escherichia coli cells," *Genetics*, vol. 149, pp. 1633–1648, 1998.

[2] J. Paulsson, O. Berg, and M. Ehrenberg, "Stochastic focusing: Fluctuation-enhanced sensitivity of intracellular regulation," *PNAS*, vol. 97, no. 13, pp. 7148–7153, 2000.

[3] D. T. Gillespie, "A rigorous derivation of the chemical master equation," *Physica A*, vol. 188, pp. 404–425, 1992.

[4] ——, "Exact stochastic simulation of coupled chemical reactions," *J. Phys. Chem.*, vol. 81, no. 25, pp. 2340–2360, May 1977.

[5] ——, "Approximate accelerated stochastic simulation of chemically reacting systems," *J. Chem. Phys.*, vol. 115, no. 4, pp. 1716–1733, Jul. 2001.

[6] Y. Cao, D. Gillespie, and L. Petzold, "The slow-scale stochastic simulation algorithm," *J. Chem. Phys.*, vol. 122, no. 014116, Jan. 2005.

[7] B. Munsky and M. Khammash, "The finite state projection algorithm for the solution of the chemical master equation," *J. Chem. Phys.*, vol. 124, no. 044104, 2006.

[8] S. Peles, B. Munsky, and M. Khammash, "Reduction and solution of the chemical master equation using time-scale separation and finite state projection," *J. Chem. Phys.*, vol. 125, no. 204104, Nov. 2006.

[9] B. Munsky and M. Khammash, "A multiple time interval finite state projection algorithm for the solution to the chemical master equation," *J. Comp. Phys.*, vol. 226, no. 1, pp. 818–835, 2007.

[10] K. Burrage, M. Hegland, S. Macnamara, and R. Sidje, "A krylov-based finite state projection algorithm for solving the chemical master equation arising in the discrete modelling of biological systems," *Proc. of The A.A.Markov 150th Anniversary Meeting*, pp. 21–37, 2006.

[11] T. Gardner, C. Cantor, and J. Collins, "Construction of a genetic toggle switch in escherichia coli," *Nature*, vol. 403, pp. 339–242, 2000.

[12] B. Munsky and M. Khammash, "Precise transient analysis of switches and trajectories in stochastic gene regulatory networks," *Submitted to IET Systems Biology*, 2008.